



# Impact of hurricanes Irma and Maria on the Pacific Tsunami Warning Center initial tsunami warning capability for the Caribbean region

Victor Sardina<sup>1</sup>, David Walsh<sup>1</sup>, Kanoa Koyanagi<sup>1</sup>, Stuart Weinstein<sup>1</sup>, Nathan Becker<sup>1</sup>, Charles McCreery<sup>1</sup>, and Christa von Hillebrandt-Andrade<sup>2</sup>

<sup>1</sup>Pacific Tsunami Warning Center, NOAA, US National Weather Service, Honolulu, Hawaii

<sup>2</sup>US NWS Caribbean Tsunami Warning Program, Mayagüez, Puerto Rico

**Correspondence:** Victor Sardina (victor.sardina@noaa.gov)

Received: 11 March 2019 – Discussion started: 19 March 2019

Revised: 10 July 2019 – Accepted: 23 July 2019 – Published: 26 August 2019

**Abstract.** In September 2017, hurricanes Irma and Maria wreaked havoc across the Caribbean region. While obliterating the infrastructure in the Caribbean nations found along their path, both hurricanes gradually destroyed the existing seismic networks. We quantified the impact of the hurricanes on the Pacific Tsunami Warning Center (PTWC) initial tsunami warning capability for the Caribbean region relying on the computation of theoretical earthquake detection and response times after accounting for hurricane-related station outages. The results show that the hurricanes rendered 38 % of the 146 stations available in the Caribbean inoperative. Within the eastern Caribbean region monitored by PTWC the hurricanes exacerbated outages to an astonishing 82 % of the available 76 seismic stations. Puerto Rico, the Virgin Islands, and the Lesser Antilles suffered the brunt of both hurricanes, and their seismic networks nearly disappeared. The double punch delivered by two successive category 5 hurricanes added up to 02:43 and 04:33 min to the earthquake detection and response times, effectively knocking out PTWC's local tsunami warning capabilities in the region. Emergency adjustments, including the temporary reduction of the number of stations required for earthquake detection and  $M_L$  magnitude release, enabled a faster response to earthquakes in the region than otherwise possible in the aftermath of hurricanes Irma and Maria.

## 1 Introduction

Two category 5 hurricanes on the Saffir–Simpson scale wreaked havoc across the Caribbean region in September 2017. Tropical storm Irma appeared near Cabo Verde, off the coast of West Africa on 30 August 2017. By 6 September 2017, Irma had already intensified to a category 5 hurricane, with maximum sustained winds peaking at  $295 \text{ km h}^{-1}$ . It continued moving westward as a category 5 hurricane causing catastrophic damage in Barbuda, Saint Barthélemy, Saint Martin, Anguilla, and the Virgin Islands. On 10 September, Irma veered north, towards the strait of Florida, after battering the northern coast of eastern and central Cuba, still as a category 5 hurricane. Less than a week later, on 16 September, tropical storm Maria developed to the east of the Lesser Antilles. By 18 September, in less than 2 d, Maria had intensified to a category 5 hurricane right before making landfall in Dominica, where it obliterated everything in its path. Hurricane Maria then continued moving to the northwest until it made landfall in Puerto Rico as a high-end category 4 hurricane on 20 September. Its path along Puerto Rico followed a diagonal trajectory that inflicted catastrophic damage to an infrastructure already left in tatters after hurricane Irma just 2 weeks prior. Meanwhile, in Hawaii, the on-duty scientists at the Pacific Tsunami Warning Center (PTWC) witnessed how most of the seismic data streams coming in from the eastern Caribbean gradually disappeared in a matter of weeks. These observations alone, however, do not sufficiently elucidate the impact of both hurricanes on tsunami warning operations. The PTWC issues its

initial tsunami messages relying entirely on the analysis of near-real-time seismic data provided by the available seismic networks, not water level data. Consequently, we quantify the impact of both hurricanes on the PTWC tsunami warning capabilities for the Caribbean by first computing the theoretical detection time of the first arriving P and S seismic waves across the region. We then manipulate these computations to generate maps illustrating the spatial distribution of the additional earthquake detection and response time delays in seconds triggered by both hurricanes.

## 2 Computational methodology

To compute the detection times of the first arriving P and S waves we rely on the procedure applied by Sardina et al. (2018a). We first apply the Tau-P method (Buland and Chapman, 1983) using the AK135 earth model (Kennett et al., 1995) via the TauP software package (Crotwell et al., 1999) and generate travel time tables for the first arriving P and S waves. We then use these tables as input to a multi-threaded C++ application written to generate 2-D grids for different combinations of receiver stations, azimuth gap constraints, and lookup regions. In all computations we place the hypocenter at 10 km, the depth reported as the most frequent for Caribbean earthquakes processed by the PTWC (Sardina et al., 2018b).

## 3 P and S wave detection times in the Caribbean

When monitoring the seismic activity within a given area geoscientists traditionally grade preliminary hypocenter determinations with smaller azimuthal gaps as having better overall quality than those with larger ones. Given both the topology of the seismic network in the Caribbean shown in Fig. 1, and its inhomogeneous density of stations, however, it turns much slower, and is therefore quite impractical for tsunami warning purposes, to set a maximum azimuthal gap restriction before releasing preliminary earthquake detections. Consequently, to locate earthquakes worldwide the PTWC teleseismic picker relies on detection of the P waves at a minimum of five stations regardless of the azimuthal gap, while the associator releases a preliminary location for further processing once it has successfully associated at least eight P picks regardless of the azimuthal gap. We mimicked the settings of the real-time monitoring system for the Caribbean by computing the detection time of the first arriving P wave at a minimum of eight stations, without azimuthal gap restrictions, after assuming that all stations provide data with minimal latency. Analysis of the distribution of the computed detection times shown in Fig. 1a reveals that by relying on detection of the first arriving P wave at the eight closest seismic stations we could detect seismic events in the Caribbean within 90 and 60 s of origin time in 83 % and 47 % of the region. Moreover, in areas covered by a denser seis-

mic network, such as Puerto Rico and the Lesser Antilles, we could detect earthquakes within 30 s of origin in 6.9 % of the region, which represents 14.7 % of the 60 s detection area.

The histogram in the upper right corner of Fig. 1b illustrates the distribution of the median latency for the seismic data streams ingested into the PTWC system. We attained these median latency values from the analysis of 628 latency log files covering the second half of 2017. We can then treat these median values as representative of the most common network status and use them as a baseline to quantify deviations from the norm. As shown in the histogram, station outages usually render 23 % (34) of the 146 stations useless, while another 52 % have data latencies longer than 10 s. We can expect only a quarter (25 %) of the stations to provide data with latencies under 10 s. The contour lines in Fig. 1b illustrate the spatial distribution of the detection time of the first arriving P wave at a minimum of eight stations once we take into account these median data latencies and station outages. Comparison of Fig. 1b to a reveals that the 90, 60, and 30 s detection areas shrink from 83 % to 54 %, 47 % to 14 %, and 6.9 % to 0.25 % of the region, thereby undergoing a 35 %, 70 %, and 96 % reduction in area.

Likewise, Fig. 2 illustrates the spatial distribution of the detection time of the first arriving S wave at a minimum of five stations, without azimuthal gap restrictions, after assuming that all stations have no data latency issues. As observed in Fig. 2a, we could detect the S waves at the five closest stations within 90, 60, and 30 s from origin time across 47 %, 18 %, and 2.7 % of the total area. Once we take into account the data latencies and station outages, however, inspection of Fig. 2b reveals that the 90, 60, and 30 s detection areas shrink from 47 % to 23 %, 18 % to 6 %, and 2.7 % to 0.2 % of the region, equivalent to a 51 %, 66 %, and 92 % reduction in area.

We further illustrate the impact of the data latencies and station outages in Fig. 3, attained by (a) subtracting the P wave detection times shown in Fig. 1a from those in Fig. 1b, and (b) subtracting the S wave detection times shown in Fig. 2a from those in Fig. 2b. As illustrated in Fig. 3a, b we can expect station outages and data latencies to cause detection delays of at least 15 s throughout at least 85 % of the Caribbean. We can also expect P and S wave detection delays of more than 30 s to affect 28 % and 34 % of the region, respectively. Longer detection delays heavily affect the northwest quadrant, including Cuba, the Cayman Islands, Jamaica, Haiti, and the Dominican Republic, due to both a more sparse seismic network to the northwest and relatively frequent station outages and longer data latencies.

Relying on detection of the P waves at the closest seismic stations without setting a maximum azimuth gap requirement results in faster earthquake detections, but also in larger azimuthal gaps. As illustrated in Fig. 4a, after taking into account the median station outages we can expect azimuthal gaps larger than 180° in 59.5 % of the Caribbean region, and across 74 % of the rectangular area monitored by the PTWC,



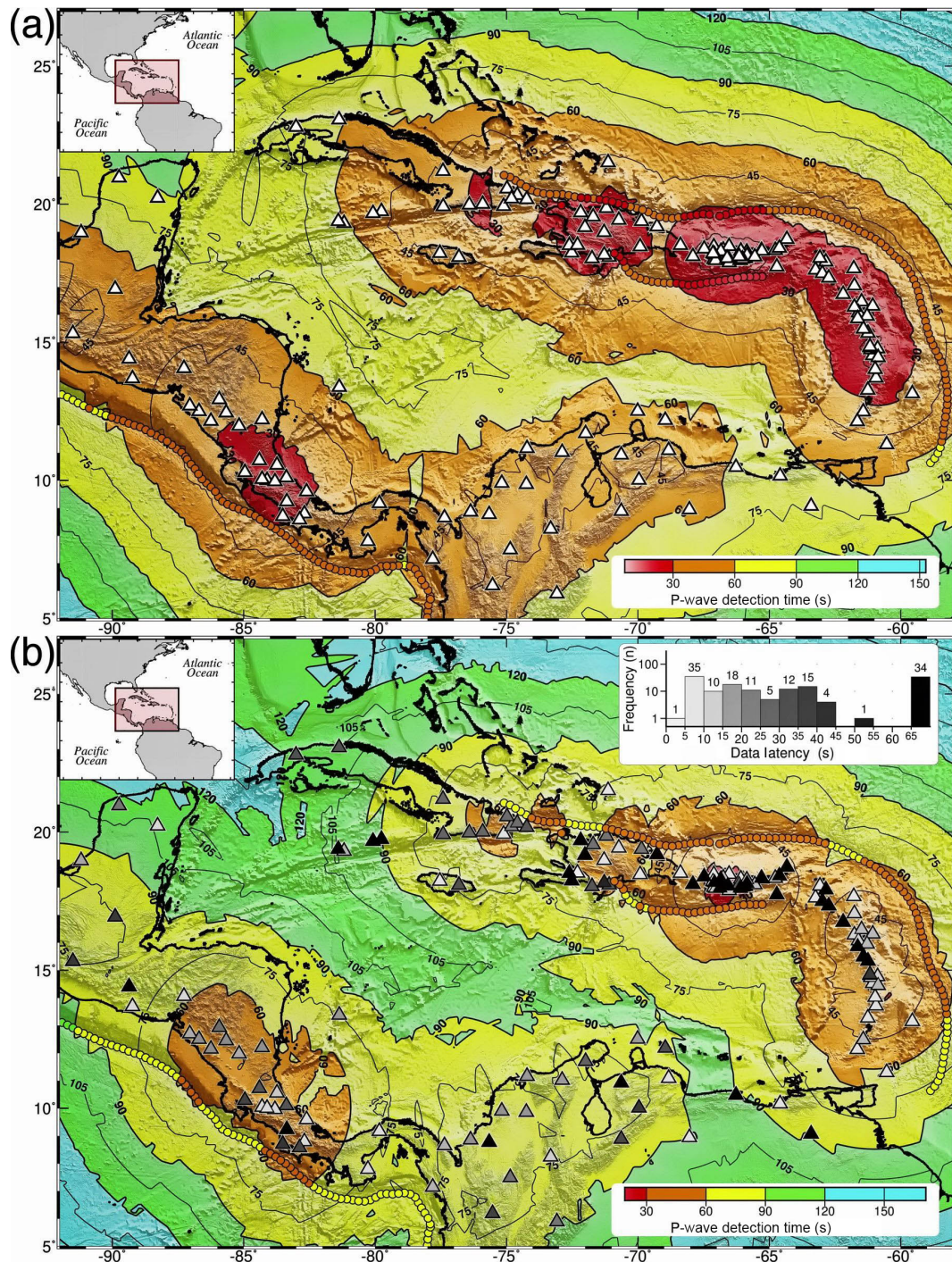


**Figure 1.** Hypothetical epicenter positions colored by the theoretical detection time of the first arriving P wave within the Caribbean region at a minimum of eight stations, regardless of azimuthal gap after (a) assuming that all seismic stations (white triangles) contribute data with no significant latencies and (b) taking into account the median data latencies and station outages. Station outages at 23 % (34 black triangles) of the 146 seismic stations and data latencies longer than 10 s for another 52 % leave only 25 % of the network with latencies under 10 s. Consequently, the 90 (yellow), 60 (orange), and 30 s (red) detection areas shrink from 83 % to 54 %, 47 % to 14 %, and 6.9 % to 0.25 % of the region, thereby undergoing a 35 %, 70 %, and 96 % reduction in area, respectively. The small, contiguous circles show the computed P wave detection times sampled every 25 km along the trench axes.



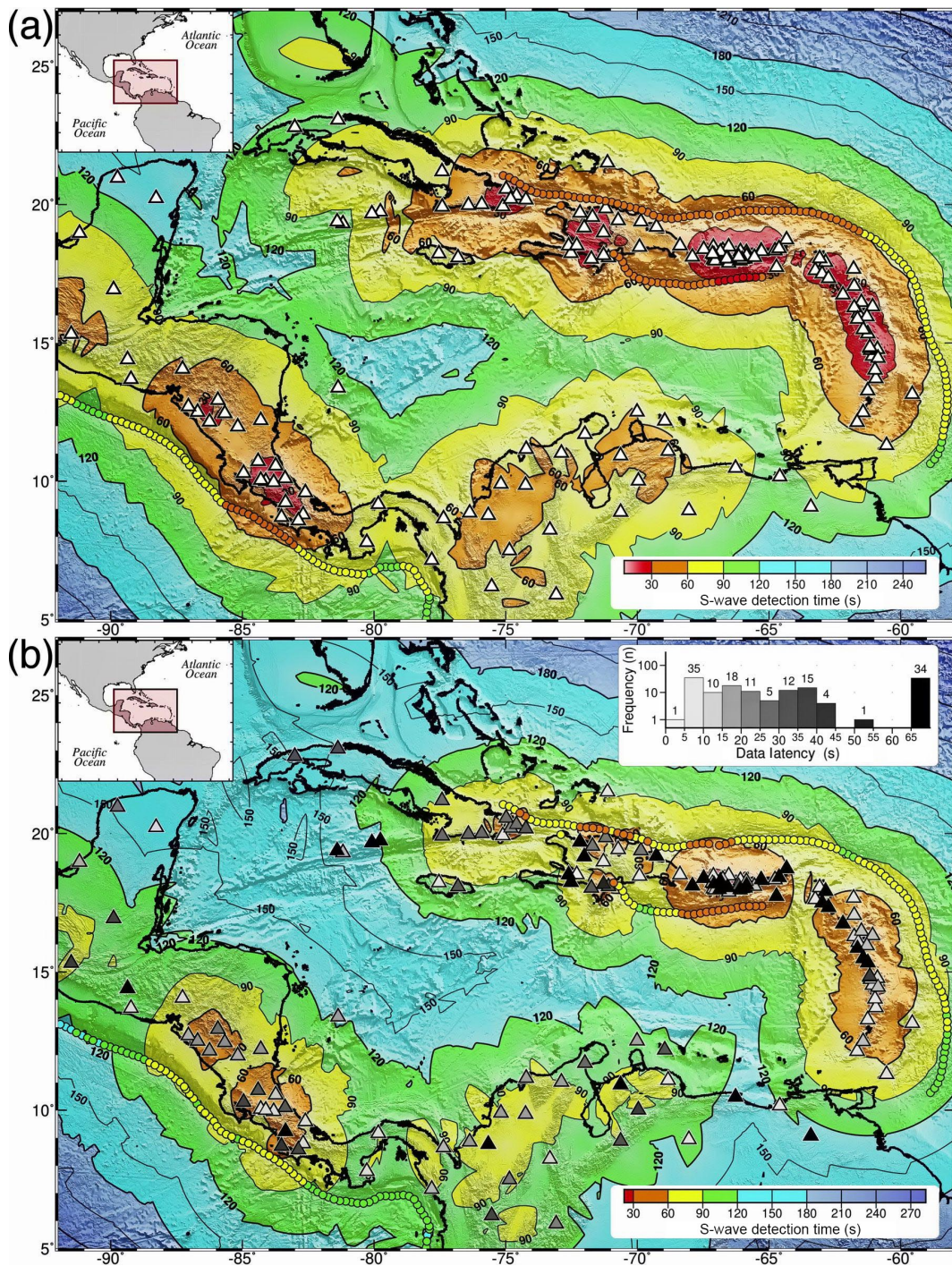


**Figure 2.** Theoretical detection time of the first arriving S wave within the Caribbean region at a minimum of five stations, regardless of azimuthal gap after (a) assuming that all seismic stations (white triangles) contribute data with no significant latencies and (b) taking into account the median data latencies and station outages. Station outages at 23 % (34 black triangles) of the 146 seismic stations and data latencies longer than 10 s for another 52 % leave only 25 % of the network with latencies under 10 s. Consequently, the 90 (yellow), 60 (orange), and 30 s (red) detection areas shrink from 47 % to 23 %, 18 % to 6 %, and 2.7 % to 0.2 % of the region, equivalent to a 51 %, 66 %, and 92 % reduction in area, respectively. The small, contiguous circles show the computed S wave detection times sampled every 25 km along the trench axes.



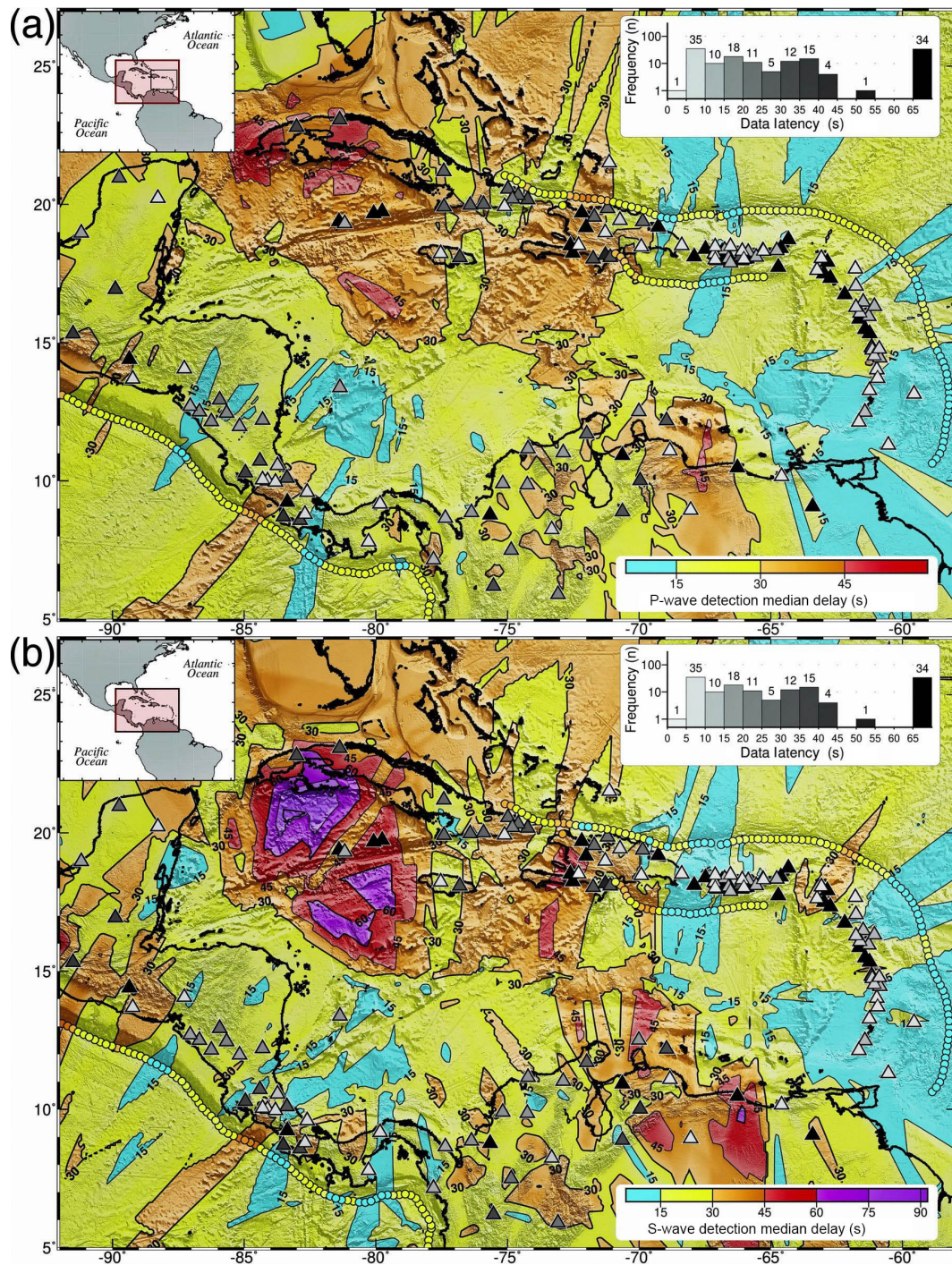


**Figure 3.** Detection delay in seconds once we account for the effect of data latencies and station outages on the detection time of the first arriving P and S waves after (a) subtracting the P wave detection times shown in Fig. 1a from those in Fig. 1b and (b) subtracting the S wave detection times shown in Fig. 2a from those in Fig. 2b. We can expect outages at 23 % (black triangles) and data latencies longer than 10 s at 52 % of the 146 stations to cause detection delays of at least 15 s across 85 % of the region. Likewise, we can expect detection delays of more than 30 s to affect 28 % and 34 % of the region in (a) and (b), respectively. The small, contiguous circles show the computed detection delays sampled every 25 km along the trench axes.

shown in more detail in Fig. 4b. When detecting earthquakes along the trench axes, to both the north and south of Puerto Rico, we can expect azimuthal gaps of more than  $270^\circ$ . These theoretical azimuthal gaps match the actual data, as for instance, during 2017 the PTWC hypocenter determinations for earthquakes in the Caribbean had azimuthal gaps characterized by a median of  $180.3^\circ$ . Despite rather large azimuthal gaps, however, the PTWC epicenter offsets had a median value of 14.3 km.

#### 4 P and S wave detection times in the Caribbean after hurricanes Irma and Maria

Hurricane Irma devastated the region's infrastructure, and this in turn contributed considerably to magnify the catastrophic damage found along the path of hurricane Maria less than 2 weeks later. The histogram in Fig. 5a illustrates the status of the Caribbean seismic network after hurricane Irma on 10 September 2017. Data outages at 53 stations now account for 36 % of all 146 stations. Comparison of Figs. 5a to 1b reveals that the 19 additional station outages attributed to Irma further reduced the 90, 60, and 30 s P wave detection areas to 47 %, 11.5 % and 0.16 % of the region, respectively. Likewise, comparison of Figs. 5b to 2b reveals that after hurricane Irma the 90, 60, and 30 s S wave detection areas shrunk to just 19.3 %, 4.8 %, and 0.1 % of the total area, respectively.

The status of the seismic monitoring for tsunami warning purposes in the Caribbean deteriorated even further less than 2 weeks later with the arrival of hurricane Maria. The histogram in Fig. 6 shows that after hurricane Maria, on 23 September 2017, the PTWC had lost access to 90 (62 %) of the 146 seismic stations available in the Caribbean, with an overwhelming number of them located in the vicinity of Puerto Rico, the Virgin Islands, and the Lesser Antilles. The paths of both hurricanes, derived from the advisories issued by the National Hurricane Center, and plotted as two white vortex tracks in all pertinent figures, match the location of the station outages. Moreover, the concentration of black triangles representing station outages in Fig. 6, for instance, underline the fact that hurricanes Irma and Maria caused an unprecedented massive blackout of the seismic networks in the eastern Caribbean.

As illustrated in Fig. 6a, after hurricane Maria, the 90 (yellow) and 60 s (orange) P wave detection areas now cover just 24.3 % and 1.35 % of the region, respectively. Likewise, Fig. 6b shows that after hurricane Maria the 90 and 60 s S wave detection areas shrunk to just 8.5 % and 0.9 % of the total area, while the 30 s detection area completely disappears for both the P and S wave detection.

We further highlight how the eastern Caribbean region suffered the brunt of both hurricanes in Figs. 7 and 8, attained by (a) subtracting the median P wave detection times shown in Fig. 1b from those after hurricane Maria shown in Fig. 5b,

and (b) subtracting the median S wave detection times shown in Fig. 2b from those after hurricane Maria shown in Fig. 6b. This essentially isolates the effect of both hurricanes on the detection times, thereby allowing us to quantify their impact as additional, hurricane-related detection delays in seconds.

As observed in Fig. 7a, when compared to normal operational conditions shown in Fig. 1b, hurricanes Irma and Maria caused additional P wave detection delays of more than 60 s (01:00) across 19 % of the Caribbean region. The longer delays, however, appear heavily concentrated within the rectangular area monitored by the PTWC in the eastern Caribbean, shown in greater detail in Fig. 7b. The combined effect of both hurricanes left just 13 stations available for seismic monitoring, with only three of them located in the Lesser Antilles. This in turn results in additional P wave detection delays of 60–163 s (01:00–02:43) across 51 % of the eastern Caribbean, including Puerto Rico, the Virgin Islands, and the Lesser Antilles.

Similarly, as illustrated in Fig. 8a, when compared to the normal operational conditions illustrated in Fig. 2b, the hurricanes caused additional S wave detection delays of 60 s (01:00) or more across 23 % of the Caribbean region. Figure 8b corroborates how the longer hurricane-triggered delays concentrate heavily within the eastern Caribbean, where additional S wave detection delays of 60–273 s (01:00–04:33) affect 60 % of the area.

#### 5 Mitigation of the impact of hurricanes Irma and Maria on P and S wave detection times

The chronic P and S wave detection delays caused by the station outages triggered by hurricanes Irma and Maria, illustrated in Fig. 6, made the eight P phase and five S phase criteria unsuitable for local tsunami warning operations. The unprecedented earthquake detection delays shown in Figs. 7 and 8 prompted emergency adjustments to the PTWC local processing system for the eastern Caribbean. As illustrated in Fig. 9, these adjustments consisted in (a) reducing the number of P phase picks required for event detection to four and (b) reducing the number of S phase picks required for preliminary  $M_L$  magnitude computation to two. While these steps improve detection times, they also result in less stable hypocenters and magnitude estimates, necessitating additional review by the on-duty geoscientists.

Relying on detection of the first arriving P wave at four stations instead of eight, however, results in a significant reduction of the impact of the hurricanes on the P wave detection times, from a maximum additional delay of 163 s (02:43) shown in Fig. 7b to the 66 s (01:06) shown in Fig. 9a. Moreover, the area affected by additional P wave detection delays of more than 60 s shrinks from 51 % in Fig. 7b to 2.7 % of the whole area in Fig. 9a, equivalent to a 95 % reduction in area.



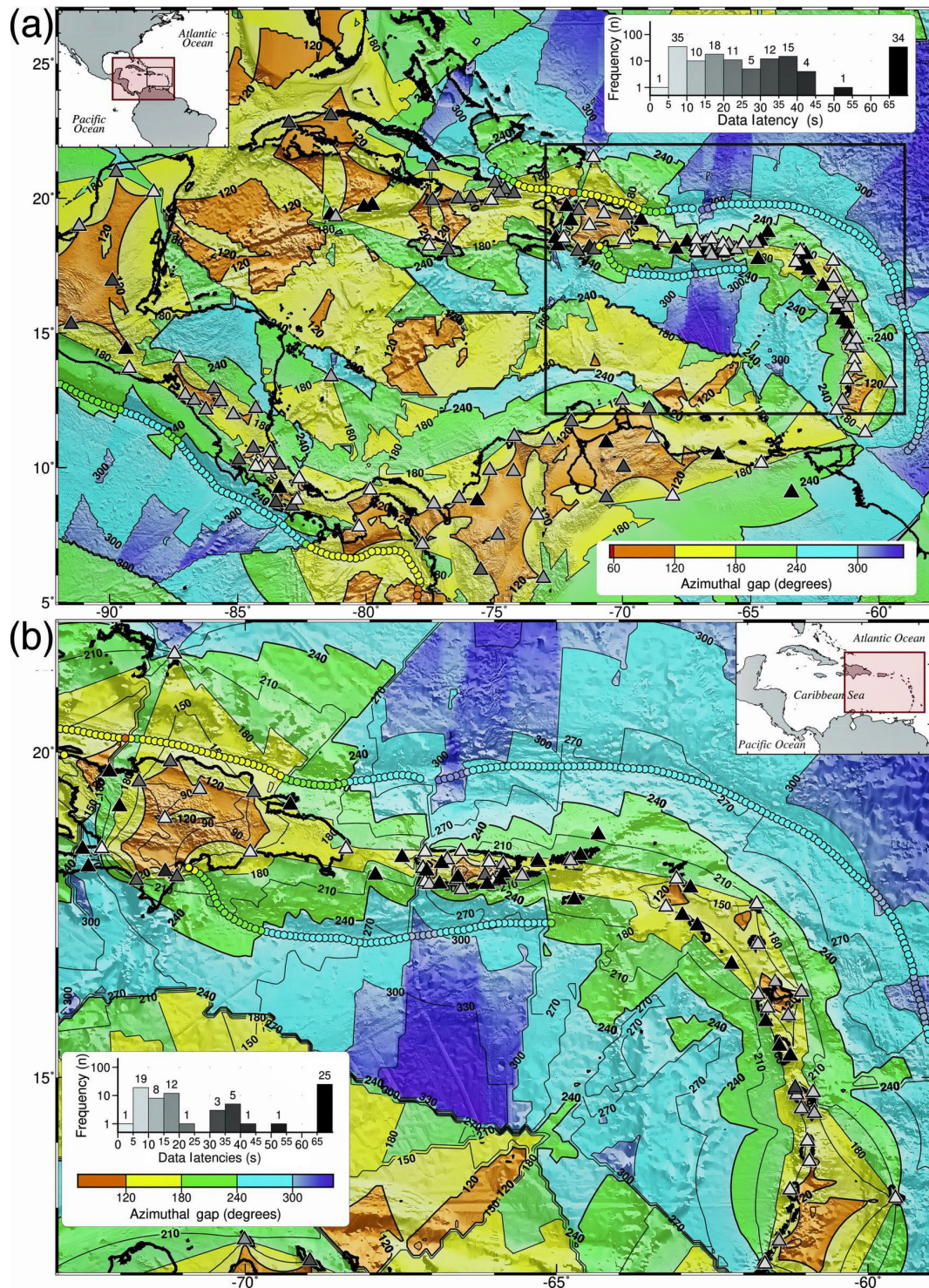


**Figure 4.** Azimuthal gap in degrees resulting from the detection of the first arriving P wave within the Caribbean at a minimum of eight stations, without azimuth gap restriction, after taking into consideration the median data latencies and station outages within (a) the Caribbean region and (b) within the rectangular area monitored by the PTWC local processing system for the eastern Caribbean. Under normal operational conditions we can expect azimuthal gaps under  $180^\circ$  (yellow) and  $120^\circ$  (orange) in just 40.5 % and 10.9 % of the Caribbean region, respectively. Within the eastern Caribbean area shown in (b) we can expect azimuthal gaps under  $180^\circ$  and  $120^\circ$  in just 26 % and 4.5 % of the total area, mostly within smaller sections located along the axis of the most densely instrumented areas.



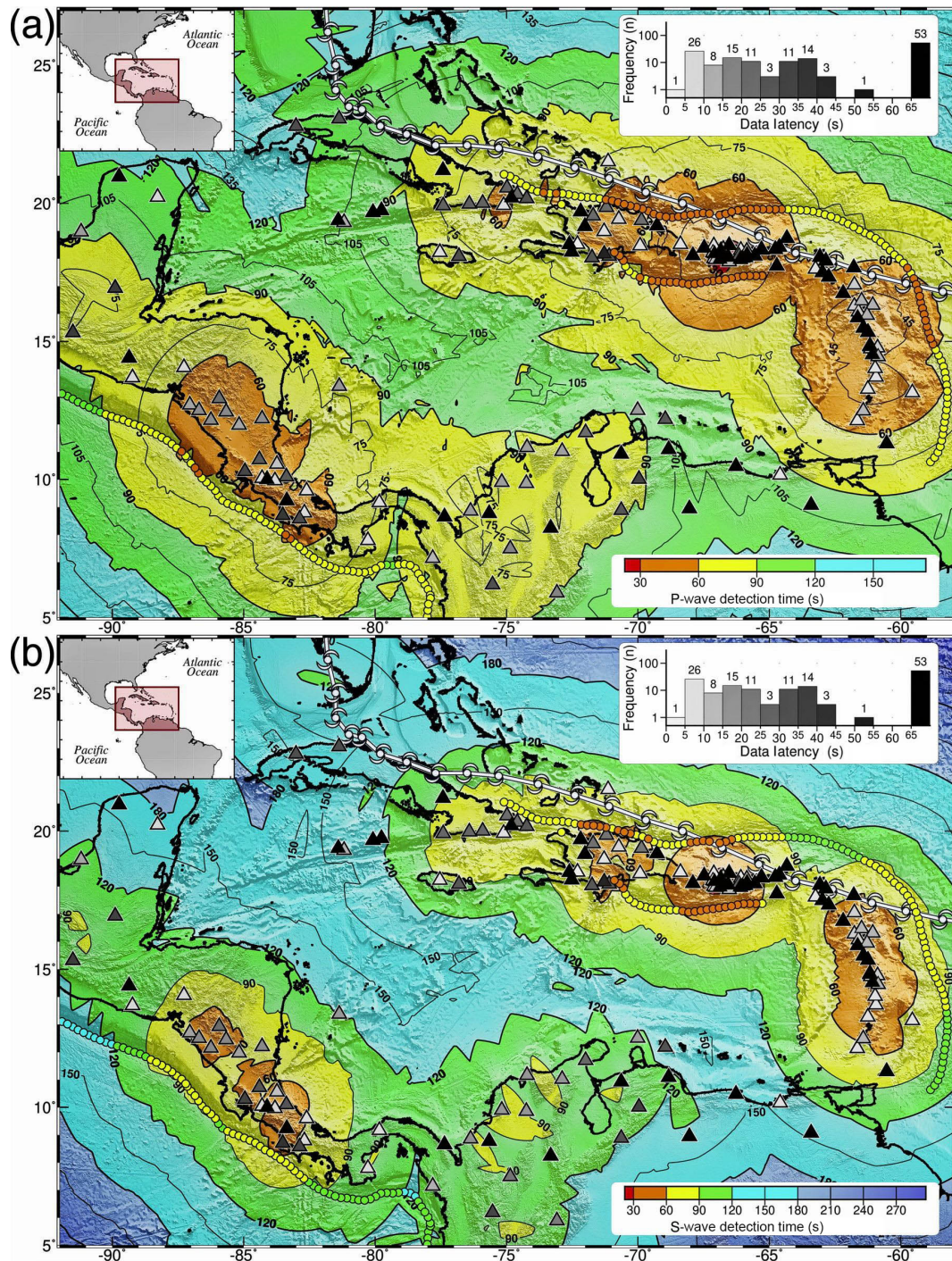


**Figure 5.** Theoretical detection time of the first arriving P and S waves in the Caribbean after hurricane Irma on 10 September 2017. The 19 additional station outages attributed to Hurricane Irma now add up to 36 % (53 black triangles) of the 146 stations. These outages in turn reduced the 90 (yellow), 60 (orange), and 30 s (red) detection areas to (a) 47 %, 11.5 %, and 0.16 % of the total area for P wave detection and (b) 19.3 %, 4.8 %, and 0.1 % of the region for S wave detection. The small, contiguous circles show the computed detection times sampled every 25 km along the trench axes. White vortex tracks show the path of hurricane Irma.



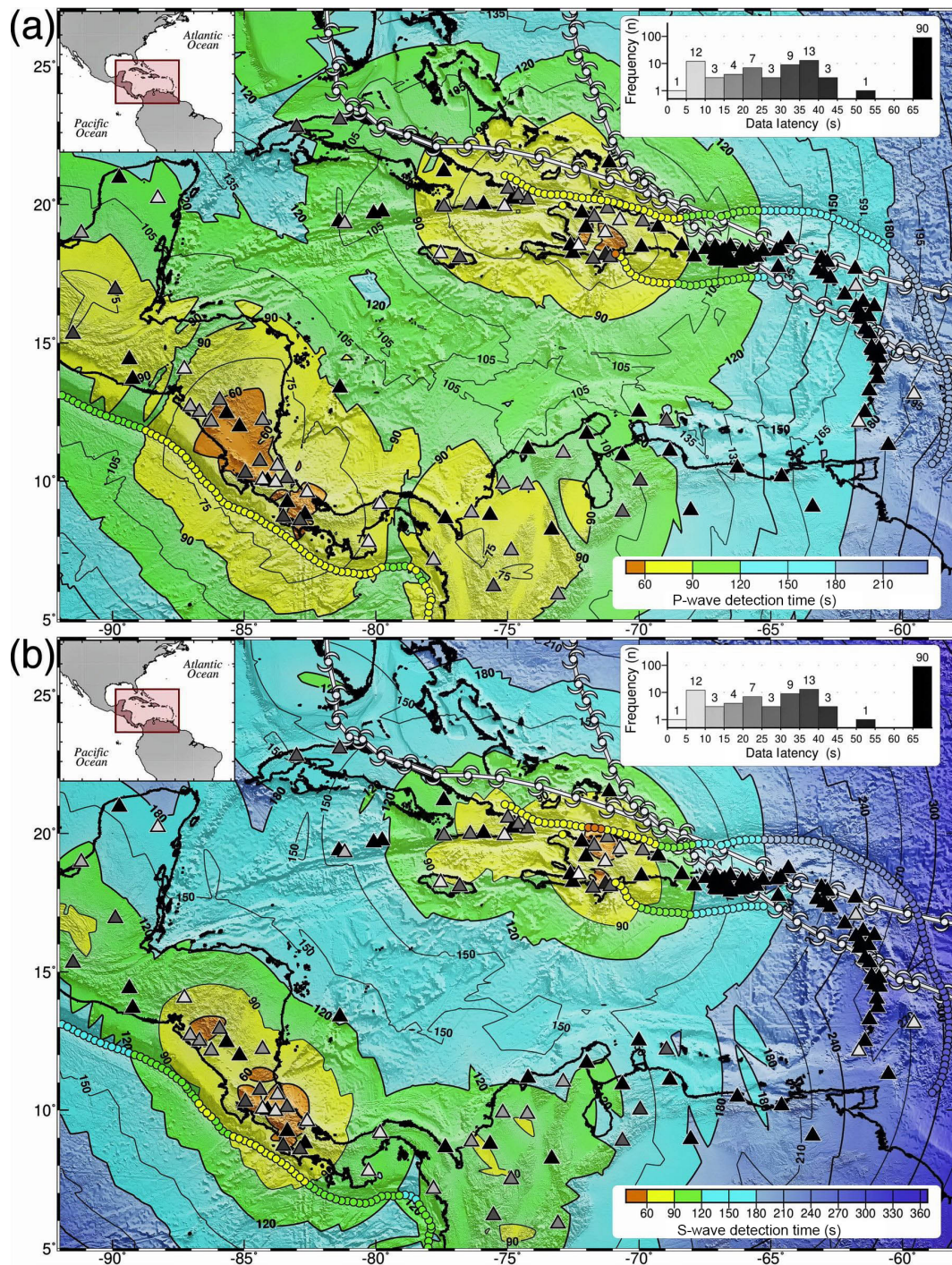


**Figure 6.** Theoretical detection time of the first arriving P and S waves in the Caribbean after hurricane Maria on 23 September 2017. The 37 additional station outages attributed to Hurricane Maria now add up to 61 % (90 black triangles) of the 146 stations. These unprecedented station outages further reduced the 90 (yellow) and 60 s (orange) detection areas to 24.3 % and 1.35 % of the region for P wave detection, and (b) 8.5 % and 0.9 % of the total area for S wave detection. The 30 s detection area disappears in both (a) and (b). The small, contiguous circles show the computed P and S wave detection times sampled every 25 km along the trench axes. White vortex tracks show the path of hurricanes Irma to the north and Maria to the south.



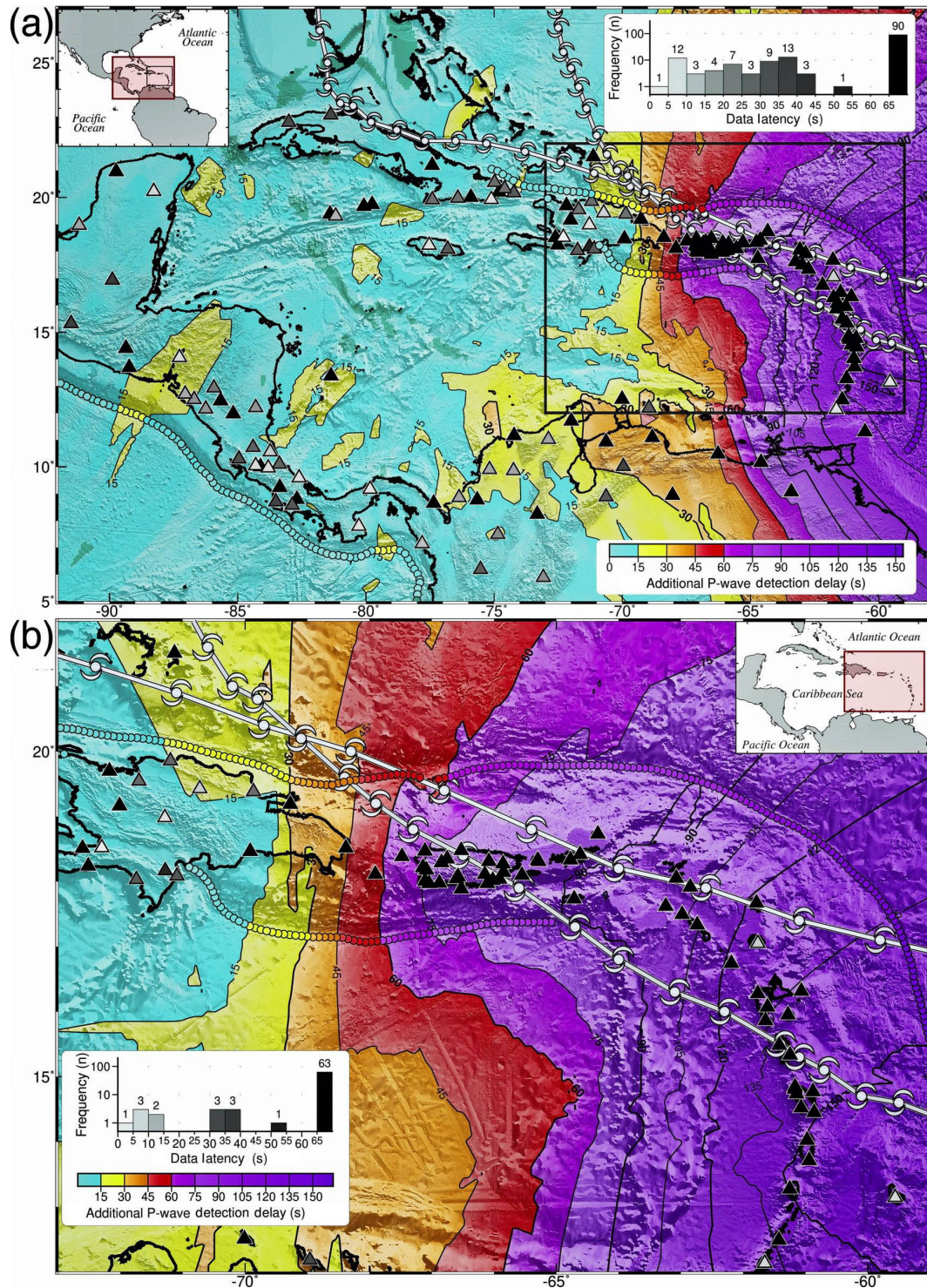


**Figure 7.** Impact of hurricanes Irma and Maria on the detection time of the first arriving P wave at a minimum of eight stations in the Caribbean after (a) subtracting the median P wave detection times shown in Fig. 1b from those in Fig. 6a and (b) zooming into the rectangular area monitored by the PTWC local processing system for the Caribbean. The hurricanes caused additional P wave detection delays of more than 15 s across 43 % of the Caribbean region. Within the eastern Caribbean shown in (b), however, additional P wave detection delays of more than 15 s affect 88 % of the total area, with delays of 60–163 s (01:00–02:43) affecting 51 % of the eastern half of the area. The small, contiguous circles show the computed P wave detection delays sampled every (a) 25 km and (b) 10 km along the trench axes. White vortex tracks show the paths of hurricanes Irma to the north and Maria to the south.



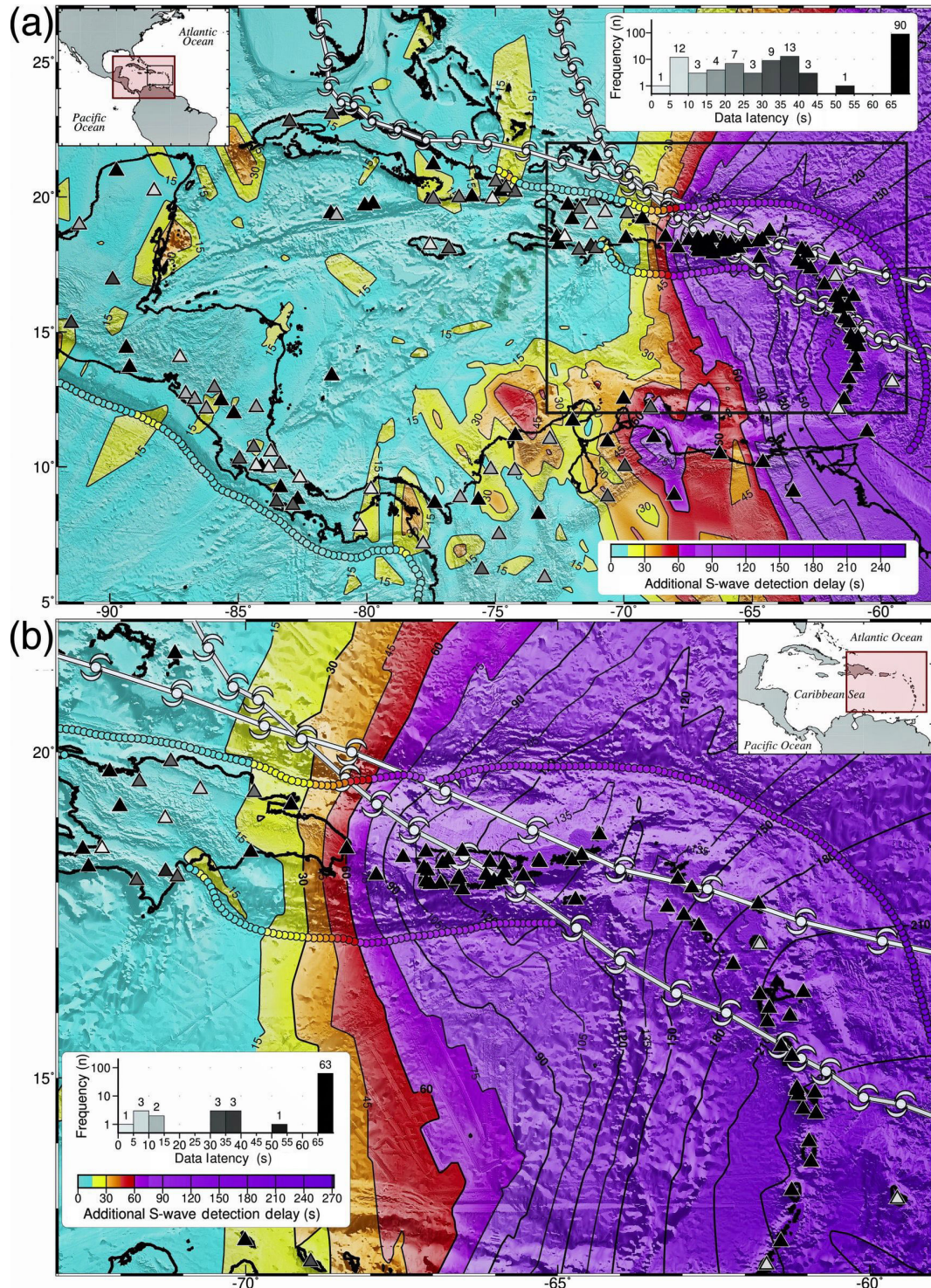


**Figure 8.** Impact of hurricanes Irma and Maria on the detection time of the first arriving S wave at a minimum of five stations in the Caribbean after (a) subtracting the median S wave detection times shown in Fig. 2b from those in Fig. 6b and (b) zooming into the rectangular area monitored by the PTWC local processing system for the Caribbean. The hurricanes caused additional S wave detection delays of more than 15 s across 45 % of the Caribbean region. Within the eastern Caribbean shown in (b), however, additional S wave detection delays of more than 15 s affect 78 % of the area, with delays of 60–273 s (00:15–04:33) affecting 61 % of the area. The small, contiguous circles show the computed S wave detection delays sampled every (a) 25 km and (b) 10 km along the trench axes. White vortex tracks show the paths of hurricanes Irma to the north and Maria to the south.



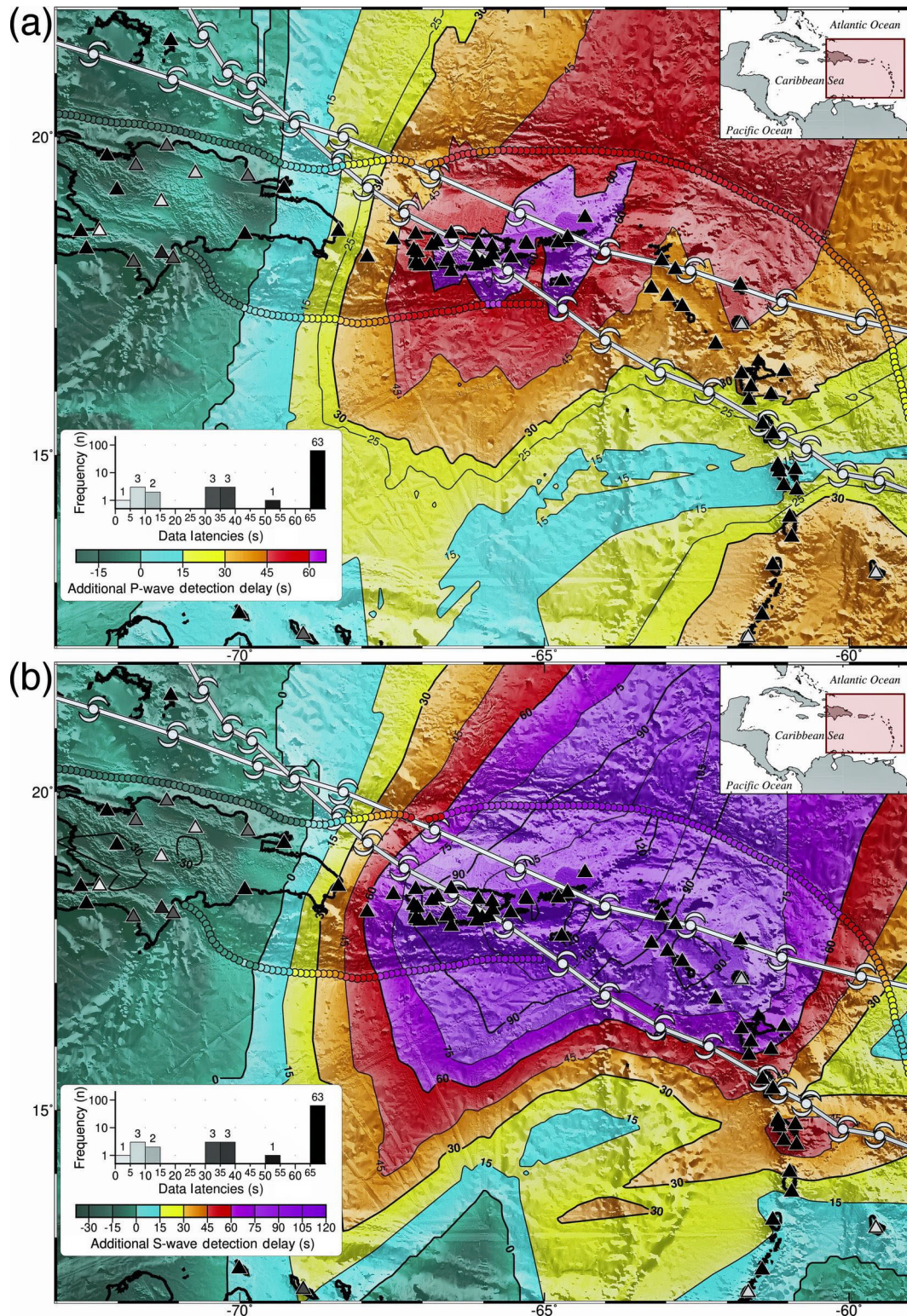
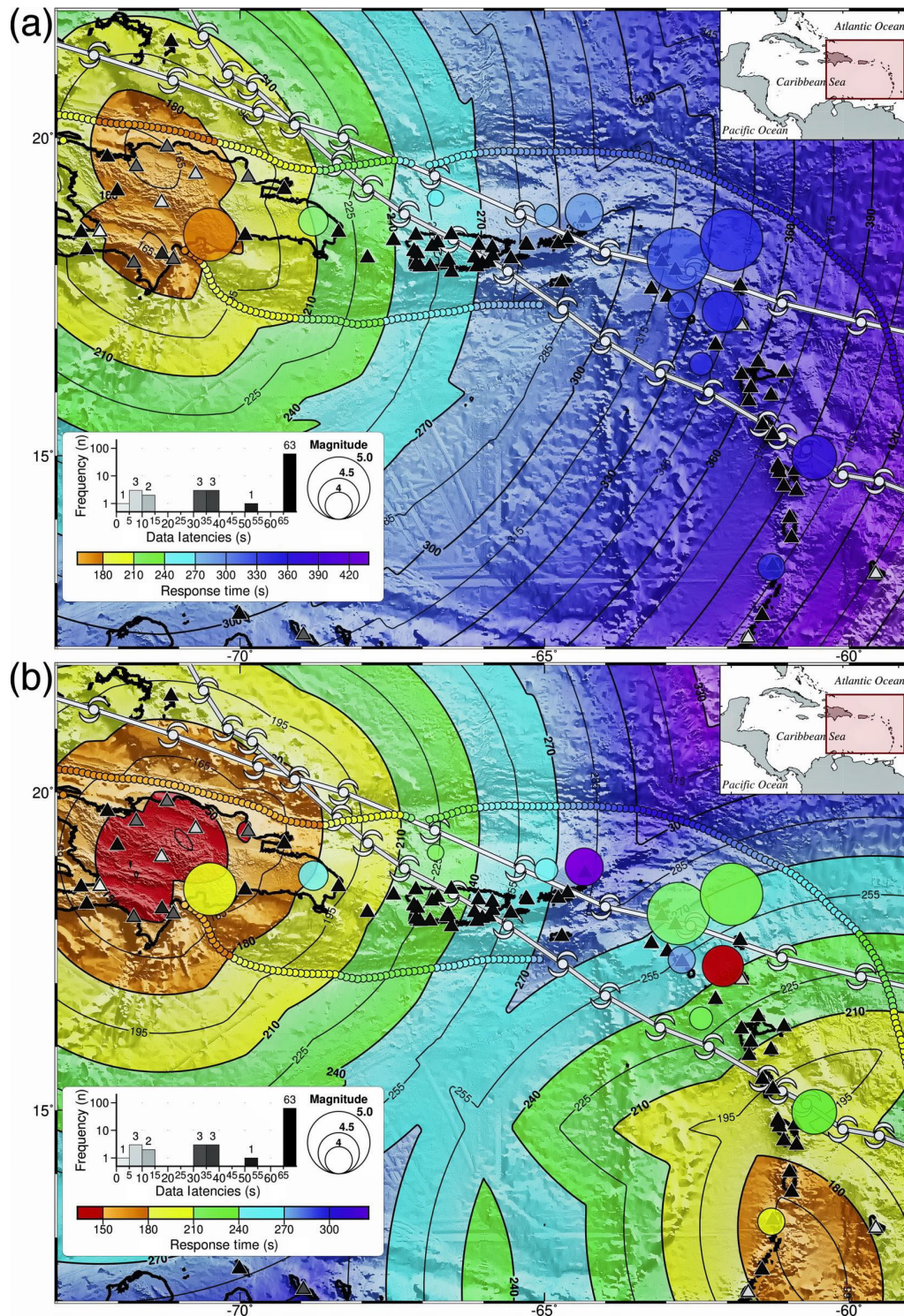


**Figure 9.** Mitigation of the impact of hurricanes Irma and Maria on the detection time of the first arriving P and S waves by (a) reducing the number of P picks required for event detection to four stations, so that we have additional P wave detection delays with a maximum of 66 instead of the 163 s (02:43) shown in Fig. 7b and (b) reducing the number of S picks required for computation and release of a preliminary  $M_L$  magnitude to two, thereby having additional S wave detection delays with a maximum of 120 instead of the 273 s (04:33) shown in Fig. 8b. The small, contiguous circles show the computed P and S wave detection delays sampled every 10 km along the trench axes. White vortex tracks show the paths of hurricanes Irma to the north and Maria to the south.





Likewise, relying on detection of the first arriving S wave at two stations instead of five for preliminary  $M_L$  computation results in a visible reduction of the impact of the hurricanes on the S wave detection times, from a maximum additional delay of 273 s (04:33) shown in Fig. 8b to the 120 s (02:00) shown in Fig. 9b. Moreover, the area affected by S wave detection delays of more than 60 s shrinks from 60 % in Fig. 8b to 30 % of the whole area in Fig. 9b, equivalent to a 50 % reduction in area.

## 6 Response times in the aftermath of hurricanes Irma and Maria

The results discussed so far underscore both how and why hurricanes Irma and Maria had the worst repercussions on tsunami warning operations in the eastern Caribbean. Consequently, when discussing their impact on the response times we will focus on the rectangular area monitored by the PTWC local monitoring system for Puerto Rico, the Virgin Islands, and the Lesser Antilles shown in Fig. 8. To illustrate the spatial distribution of the theoretical response times in the wake of both hurricanes, we converted the S wave detection maps reflecting the hurricanes' impact into theoretical response time maps by adding 110 s to account for (a) the 30 s S wave coda window required for  $M_L$  magnitude computation, and (b) the historical median of 80 s needed to review the available data and compose a message after Sardina et al. (2018b).

We computed the theoretical response times for detection of the first arriving S wave at a minimum of five stations by applying the operation Fig. 10a = (Fig. 6b + 110). As indicated by the contour lines in Fig. 10a, relying on S wave detection at a minimum of five stations leads to response times of 240–463 s (04:00–07:43) for any earthquake located to the east of the Dominican Republic. The diameter of the circles plotted in Fig. 10 indicates the magnitude of 12 local earthquakes processed by the PTWC between 12 September 2017 and 7 January 2018. Their color reflects the theoretical response time read directly from the map.

To compute the theoretical response times after detection of the first arriving S wave at a minimum of two stations we applied the operation Fig. 10b = (Fig. 2b + Fig. 8b + 110). The color assigned to the 12 earthquake symbols in Fig. 10b now indicates the actual PTWC response times using the same timescale applied to the contours. As we can observe, the color assigned to all but one earthquake differs from the color of the contour bands underneath by no more than the equivalent of  $\pm 30$  s. We can attribute these differences to (a) faster or slower manual review and message composition than the median 80 s and (b) the gradual repair and availability of more seismic stations as part of the hurricanes' recovery process. This corroborates that adjusting the settings of the monitoring system to rely on detection at four stations, plus the computation of preliminary  $M_L$  magnitudes

at two stations, considerably reduced the additional delays attributed to the impact of the hurricanes.

## 7 Conclusions

We assessed the devastating impact of hurricanes Irma and Maria on the Pacific Tsunami Warning Center (PTWC) tsunami warning capabilities for the Caribbean relying on the computation of theoretical earthquake detection and response times. In these computations we accounted for the topology of the seismic network, but also the median data latencies and the additional station outages attributed to both hurricanes in September 2017. Analysis of the results allows us to draw the following conclusions.

- Analysis of the log files documenting the latency of the seismic data streams ingested into the PTWC system from the Caribbean during the second half of 2017 reveals that under normal operational conditions we can expect (a) outages at 23 % (34) of the 146 stations, (b) data latencies exceeding 10 s for another 52 %, and (c) just a quarter (25 %) of all data streams with latencies under 10 s.
- Theoretical computation of the detection time of the first arriving P wave in the Caribbean region at a minimum of eight stations reveals that under normal operational conditions we can expect data latencies and station outages to cause P wave detection delays exceeding 15 s across 85 % of the Caribbean, with delays of 30–59 s (00:30–00:59) affecting 28 % of the region (Figs. 1 and 3a).
- Theoretical computation of the detection time of the first arriving S wave in the Caribbean region at a minimum of five stations reveals that we can expect data latencies and station outages to cause S wave detection delays of 15 s or more across 86 % of the Caribbean, with detection delays of 30–92 s (00:30–01:32) affecting 34 % of the region (Figs. 2 and 3b).
- Relying on detection of the first arriving P wave in the Caribbean region at a minimum of eight stations results in preliminary earthquake locations with azimuthal gaps of more than  $180^\circ$  across 59.5 % of the Caribbean region (Fig. 4a) and 76 % of the rectangular area monitored by the PTWC in the eastern Caribbean (Fig. 4b).
- After hurricane Irma, on 10 September 2017, the PTWC had lost access to 36 % (53) of the 146 stations available in the Caribbean. The 19 station outages attributed to hurricane Irma caused additional P and S wave detection delays that reduced the 90, 60, and 30 s detection areas to (a) 47 %, 11.5 %, and 0.16 % of the region for P wave detection and (b) 19.3 %, 4.8 %, and 0.1 % of the region for S wave detection (Fig. 5).



- After hurricane Maria, on 23 September 2017, the PTWC had lost access to 62 % (90) of the 146 stations available in the Caribbean. These unprecedented, massive seismic station outages attributed to hurricanes Irma and Maria resulted in additional P and S wave detection delays that reduced the 90 and 60 s detection areas to (a) 24.3 % and 1.35 % of the region for P wave detection and (b) 8.5 % and 0.9 % of the total area for S wave detection, while the 30 s detection area completely disappeared (Fig. 6).
- The hurricanes caused additional P and S wave detection delays of more than 15 s across 43 % and 45 % of the Caribbean region (Figs. 7a and 8a), respectively. The longest detection delays, however, concentrate heavily along the path of both hurricanes in the eastern Caribbean, where additional P and S wave detection delays exceeding 15 s affect 88 % and 78 % of the area, respectively. Moreover, within the rectangular area monitored by the PTWC, P wave detection delays of 60–163 s (01:00–02:43) affect 51 % of the area (Fig. 7b), while S wave detection delays of 60–273 s (01:00–04:33) affect 61 % of the area (Fig. 8b).
- Computation of the theoretical response times for the eastern Caribbean while accounting for the impact of hurricanes Irma and Maria results in response times of 240–463 s (04:00–07:43) for any earthquake located to the east of the Dominican Republic (Fig. 10a). The theoretical response times based on the detection of the S waves at a minimum of two stations, however, show good agreement with the actual PTWC response times for 12 events processed between 12 September 2017 and 7 January 2018, within  $\pm 30$  s (Fig. 10b). This corroborates that adjusting the monitoring system to rely on detection of the first arriving P wave at four stations instead of eight for event location, plus detection of the first arriving S wave at two instead of five stations to compute preliminary  $M_L$  magnitudes, considerably reduced the additional message delays attributed to the impact of the hurricanes (Fig. 10b).
- Theoretical computation and analysis of the impact of the additional station outages attributed to hurricanes Irma and Maria on the detection and response times in the Caribbean reveals that after hurricane Maria the PTWC no longer had a local tsunami warning capability for Puerto Rico and the Virgin Islands. The massive blackout of seismic stations in the eastern Caribbean made it operationally impractical to either detect and locate local earthquakes or compute  $M_L$  magnitudes as low as 3.8 in a timely manner. Notwithstanding, the PTWC still maintained a regional tsunami warning capability for the Caribbean, including Puerto Rico and the Virgin Islands, relying on its teleseismic monitoring system for the region, albeit for magnitude 6.0 or

larger magnitude earthquakes, and response times quite likely to exceed 6 min for events located in the eastern Caribbean.

- The devastating impact of hurricanes Irma and Maria on the PTWC local tsunami warning capabilities for Puerto Rico and the Virgin Islands highlights the vital and potentially life-saving role of educating the population to self-evacuate in the event of prolonged or strong ground shaking instead of waiting for official tsunami messages.
- When reinstalling damaged stations and rebuilding the supporting infrastructure, network operators should consider hurricane-proofing at least a subset of their seismic stations, so as to maintain a minimum earthquake monitoring and local tsunami warning capability even if impacted by category 5 hurricanes such as Irma and Maria. To facilitate station selection, a compilation of usage statistics combined with the generation of theoretical detection and response time maps as performed in this study should reveal the stations most valuable to any regional monitoring network.

*Data availability.* No data sets were used in this article.

*Author contributions.* VS conceived the original paper scope and methodology, wrote the required C++ source code and bash scripts, compiled the supporting data, generated the figures via GMT, and wrote and edited the original draft. DW provided access to the latency logs for the seismic data streams and reviewed the paper. KK provided information about the local seismic processing system and contributed to the paper. SW, CM, and CH reviewed the paper and provided feedback on the results. NB assisted with the GMT-related scripts.

*Competing interests.* The authors declare that they have no conflict of interest.

*Acknowledgements.* In this study we used the TauP software package (Crotwell et al., 1999) to generate travel time tables for the first arriving P and S waves. We also used the Qt C++ framework (<https://www.qt.io>, last access: February 2018) to further develop the multithreaded C++ application used to generate the 2-D travel time grids subsequently manipulated and plotted via the Generic Mapping Tools (GMT) (Wessel et al., 2013) software package. We retrieved the hurricane path data from the National Hurricane Center (NHC), 2017 Tropical Cyclone Advisory Archive online at <https://www.nhc.noaa.gov/archive/2017> (last access: February 2018).



*Review statement.* This paper was edited by Maria Ana Baptista and reviewed by Ocal Necmioglu, Francois Schindele, and one anonymous referee.

## References

- Buland, R. and Chapman, C. H.: The computation of seismic travel times, *B. Seismol. Soc. Am.*, 73, 1271–1302, 1983.
- Crotwell, H. P., Owens, T. J., and Ritse, J.: The TauP Toolkit: Flexible seismic travel-time and ray-path utilities, *Seismol. Res. Lett.*, 70, 154–160, 1999.
- Kennett, B. L., Engdahl, E. R., and Buland, R.: Constraints on seismic velocities in the Earth from travel times, *Geophys. J. Int.*, 122, 108–122, 1995.
- Sardina, V., Koyanagi, K., Becker, N., Walsh, D., McCreery, C., Weinstein, S., and von Hillebrandt-Andrade, C.: Assessment of the Pacific Tsunami Warning Center's Capabilities for Puerto Rico and the Virgin Islands based on the Computation of Detection and Response Times Accounting for Seismic Network Topology and Data Latencies, *Seismol. Res. Lett.*, 89, 424–431, 2018a.
- Sardina, V., Koyanagi, K., Becker, N., Walsh, D., McCreery, C., Weinstein, S., and von Hillebrandt-Andrade, C.: Evaluation of the Pacific Tsunami Warning Center's Performance for the Caribbean based on the Compilation and Analysis of Tsunami Messages issued between 2003 and July, 2017, *Seismol. Res. Lett.*, 89, 416–423, 2018b.
- Wessel, P., Smith, W. H. F., Scharroo, R., Luis, J. F., and Wobbe, F.: Generic Mapping Tools: Improved version released, *Eos Trans. AGU*, 94, 409–410, 2013.